Supporting Information

Crumpled Graphene Balls-Based Broadband Solar Absorber

Wei Hao, Kevin Chiou, Yiming Qiao, Yanming Liu, Chengyi Song, Tao Deng and Jiaxing Huang**

1. Simulation of the Reflection of CGB Thin Film

Optical property of graphene

The absorption coefficient of a single layer graphene is πα. The optical transmission T and reflection R could be calculated by Equation S1 and Equation S2.

$$T = (1 + \frac{1}{2}\pi\alpha)^{-2} \quad \text{(S1)}$$

$$R = \frac{1}{4}\pi^2\alpha^2 T \quad \text{(S2)}$$

where $\alpha = 2\pi e^2/hc \approx 1/137$, e is the electron charge, c the light velocity, and h the Planck's constant.[4] The reflection of the single layer graphene (0.013%) is relatively small compared with the absorption (2.3%). Considering the multilayer graphene with N (less than 6) layers, the absorption coefficient is Nπα and the reflection coefficient of multilayer graphene is also small. For the graphene film that has more than 10

layers, the reflection coefficient will increase since the optical path in these layers cannot be neglected.[1]

Calculation of Mie coefficient

A set of Matlab functions, which are based on the formulation of Bohren and Huffman, are used for Mie calculations.[2] The time variation in the function is assumed as exp(-iωt), which will result in a positive imaginary parts in the composite refractive index. The key coefficients a_n and b_n, which describe the scattered field, can be calculated by Equation S3 and Equation S4. The coefficients of the internal field c_n and d_n are given by Equation S5 and Equation S6.

$$a_n = \frac{\mu m^2 j_n(mx)\left[x j_n(x)\right]' - \mu_1 j_n(x)\left[mx j_n(mx)\right]'}{\mu m^2 j_n(mx)\left[x h_n^{(1)}(x)\right]' - \mu_1 h_n^{(1)}(x)\left[mx j_n(mx)\right]'} \quad \text{(S3)}$$

$$b_n = \frac{\mu_1 j_n(mx)\left[x j_n(x)\right]' - \mu j_n(x)[mx j_n(mx)]'}{\mu_1 j_n(mx)\left[x h_n^{(1)}(x)\right]' - \mu h_n^{(1)}(x)[mx j_n(mx)]'} \quad \text{(S4)}$$

$$c_n = \frac{\mu_1 j_n(x)\left[x h_n^{(1)}(x)\right]' - \mu_1 h_n^{(1)}(x)[x j_n(x)]'}{\mu_1 j_n(mx)\left[x h_n^{(1)}(x)\right]' - \mu h_n^{(1)}(x)[mx j_n(mx)]'} \quad \text{(S5)}$$

$$d_n = \frac{\mu_1 m j_n(x)\left[x h_n^{(1)}(x)\right]' - \mu_1 m h_n^{(1)}(x)[x j_n(x)]'}{\mu m^2 j_n(mx)\left[x h_n^{(1)}(x)\right]' - \mu_1 h_n^{(1)}(x)[mx j_n(mx)]'} \quad \text{(S6)}$$

where index n changes from 1 to $n_{max} = x + 4x^{1/3} + 2$. x is the size parameter that equals to $2\pi a/\lambda$, where a is the radius of the spherical particles and λ is the light wavelength in the ambient medium. μ and μ_1 are the permeability of the ambient medium and spherical particle, respectively. $m = (\varepsilon_1\mu_1)^{1/2}/(\varepsilon\mu)^{1/2}$ and it is the refractive index of ambient medium. ε and ε_1 are the permittivity of the ambient

medium and spherical particle. The functions $j_n(z)$ and $h_n^{(1)}(z) = j_n(z) + iy_n(z)$ are spherical Bessel functions of order n.

Calculation of Mie Efficiencies

The Mie efficiencies Q_i for the interaction between light and the spherical particle are defined as the radiation interaction normalized to the cross section (σ) of the spherical particle, with radius of a as shown in Equation S7:

$$Q_i = \frac{\sigma_i}{\sigma_g} \tag{S7}$$

where $\sigma_g = \pi a^2$. Q_i is placeholder for efficiencies of extinction, absorption, or scattering with i being sca, ext or abs, respectively.

The scattering efficiency Q_{sca} includes the integration of scattered power at all directions and can be calculated by Equation S8. The extinction efficiency Q_{ext} is calculated by the extinction theorem of van de Hulst (Equation S9).[3] After obtaining Q_{sca} and Q_{ext}, the absorption efficiency Q_{abs} can be calculated through the energy conservation (Equation S10) shows.

$$Q_{sca} = \frac{2}{x^2}\sum_{n=1}^{\infty}(2n+1)(|a_n|^2 + |b_n|^2) \tag{S8}$$

$$Q_{ext} = \frac{2}{x^2}\sum_{n=1}^{\infty}(2n+1)Re(a_n + b_n) \tag{S9}$$

$$Q_{abs} = Q_{ext} - Q_{sca} \tag{S10}$$

Furthermore, the asymmetry parameter g=$\langle cos\theta \rangle$ was defined as the average cosine of the scattering angle θ with respect to power (Equation S11).

$$Q_{sca}\langle cos\theta\rangle = \frac{4}{x^2}\left\{\sum_{n=1}^{\infty}\frac{n(n+2)}{n+1}Re\left(a_n a_{n+1}^{*} + b_n b_{n+1}^{*}\right) + \sum_{n=1}^{\infty}\frac{2n+1}{n(n+1)}Re\left(a_n b_n^{*}\right)\right\} \quad \text{(S11)}$$

Calculation of Material Properties

We assumed that in the thin film, the CGBs are close packed and the interspace is filled by air. Thus, the absorption and scattering properties of CGB films could be calculated by integrating the absorption and scattering efficiency.

$$\Sigma_{abs} = N\pi a^2 Q_{abs} \quad \text{(S12)}$$

$$\Sigma_{sca} = N\pi a^2 Q_{sca} \quad \text{(S13)}$$

where Σ_{abs} and Σ_{sca} are the absorption and scattering parameter. N is the number of spherical particle in the unit volume (1 mm^3), which could be calculate from the particle radius and packing geometry. With the asymmetry parameter $g = < cos\theta >$, which indicates the average cosine of the scattering angle θ with respect to power, we can define the bulk scattering property of the material.

The model we set for the tracepro simulation is a thin film with thickness of 78 μm and radius of 10 mm. Uniform light flux with light intensity of one sun is illuminated on the surface of the thin film and detectors are placed above and below the thin film to measure the reflection and transmission. The reflection distributions at different wavelengths are shown in the supplementary Figure S3.

2. Evaporation Efficiency Details

The heat loss of the r-GO and CGB films could be estimated from three major contributions that include radiation, convection and conduction. These terms can be calculated using the Equation S14, Equation S15 and Equation S16:

$$q_{rad} = \varepsilon\sigma\left(T^4 - {T_0}^4\right) \quad \text{(S14)}$$

$$q_{conv} = h\left(T - T_0\right) \quad \text{(S15)}$$

$$q_{cond} = k\frac{dT}{dx} \quad \text{(S16)}$$

where, q_{rad}, $q_{conv,}$ and q_{cond} are the heat losses of radiation, convection and conduction, respectively. ε is the emissivity of the thin films, σ is the Stefan-Boltzmann constant, T is the temperature of the thin films, T_0 is the temperature of atmosphere, h is heat transfer coefficient and assumed to be 5 W m^{-2} K^{-1}, k is the thermal conductivity of expandable polyethylene (EPE) foam (0.032 W m^{-1} K^{-1}), and dT/dx is the thermal gradient.

The CGB800 film was illuminated at light density of 1088 W m^{-2}, and the emissivity ε of CGB800 film is 0.96. The average temperature of the CGB800 film was 39.4 °C. The heat loss through radiation was calculated to be 71.6 W m^{-2} and the heat loss of convection was 57.0 W m^{-2}. The thermal gradient was estimated through the measured temperature deference and the resulting heat loss through conduction was 8.8 W m^{-2}. With the evaporation efficiency of 84.6%, the total heat consumed in the evaporation process was ~97.2% of the input light energy, which was close to the measured absorption of CGB800 film (97.4%).

For the r-GO film, the light density and emissivity were the same with the CGB800 film. The average temperature of the r-GO film was 37.7 °C. The heat loss of radiation is 60.4 W m^{-2} and the heat loss of convection is 48.5 W m^{-2}. The heat loss through conduction is 7.5 W m^{-2}. With the evaporation efficiency of 70.8%, the total

heat consumed was ~81.5% of the input light energy, which was close to the average absorption of r-GO film (84.3%).

3. Porosity of Crumpled Graphene Ball and rGO samples

Gas sorption analyzer (Autosorb iQ, Quantachrome Instruments U.S.) was used to measure the porosity of the CGB800 and rGO and the test data were showed as figure S7. Through the analysis of the data with Brunauer–Emmett–Teller (BET) method, the porosity of CGB800 sample is 1.14 cm^3/g, which is much larger than that of the rGO sample (0.17 cm^3/g).

4. Supplementary Figures

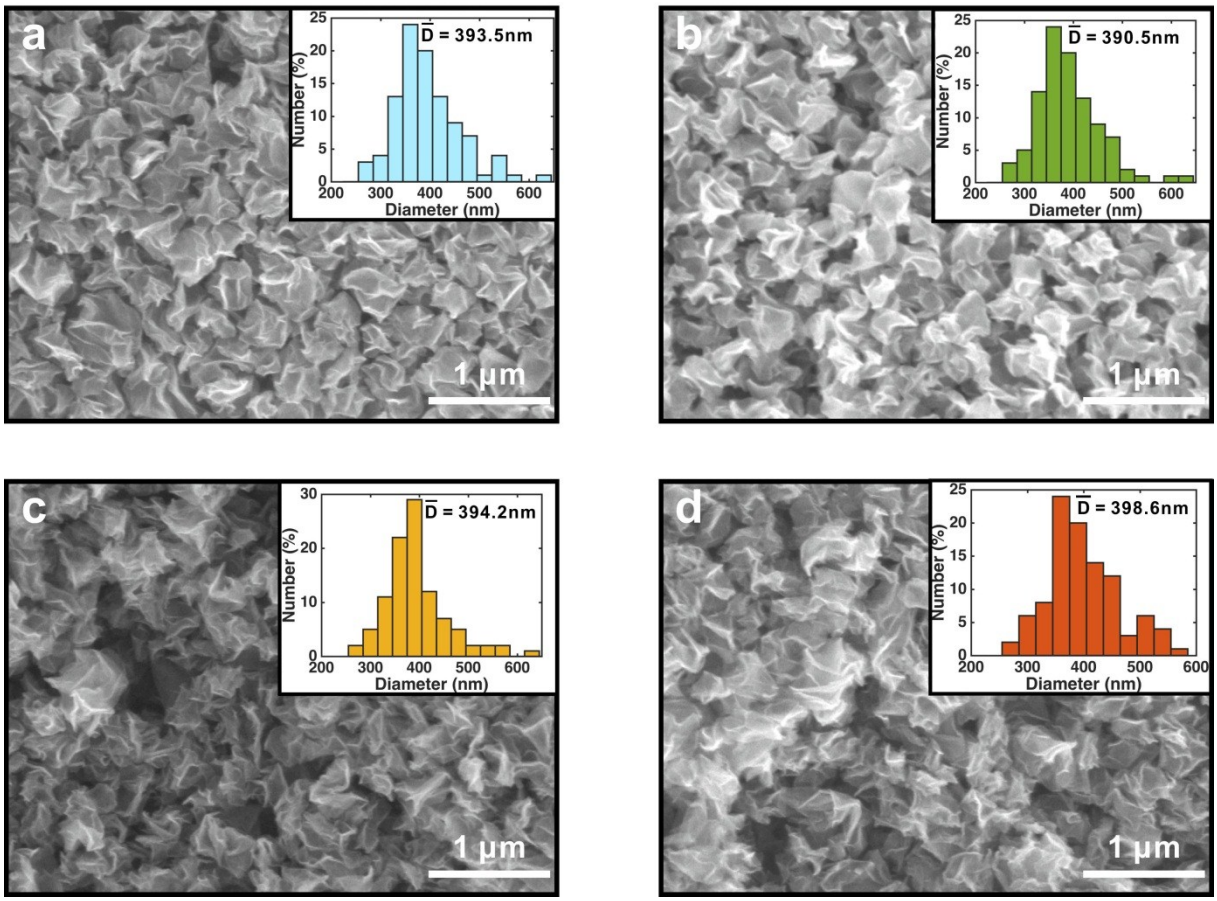

Figure S1. SEM images and size distributions of (a) CGB500 film, (b) CGB600 film, (c) CGB700 film, and (d) CGB800 film

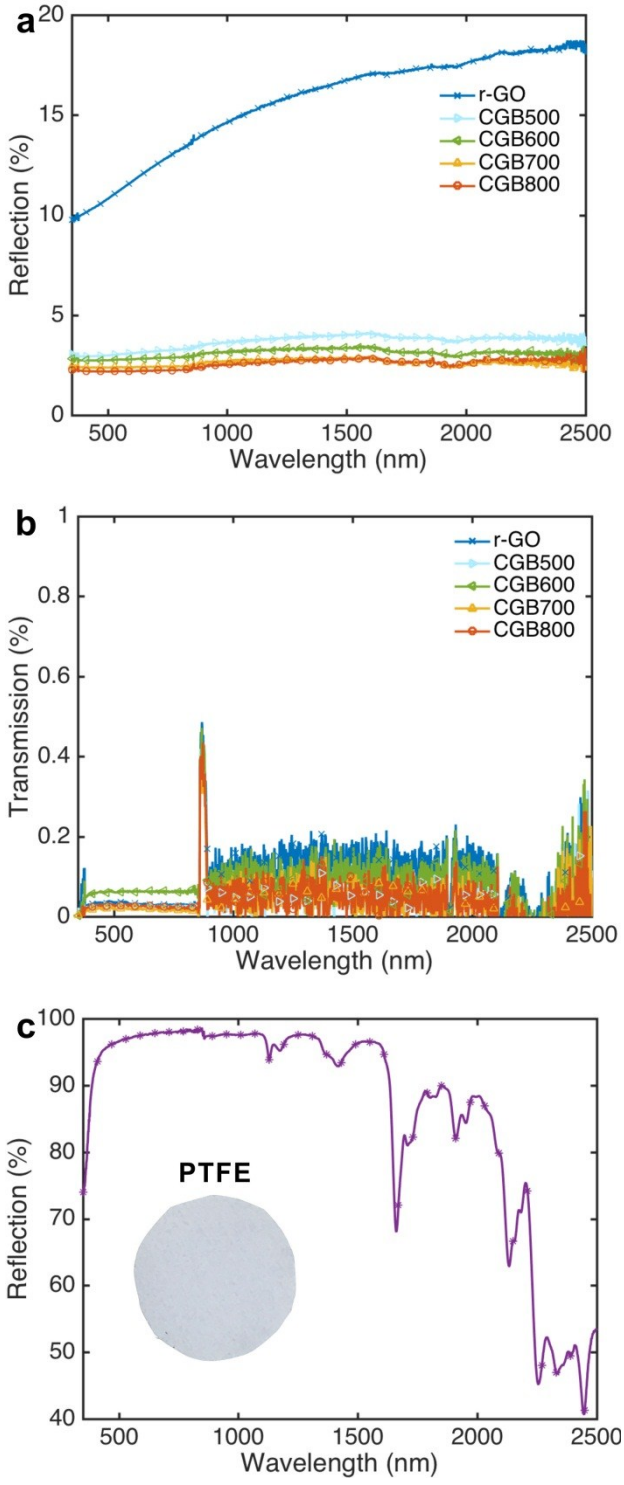

Figure S2. UV-VIS-NIR (a) Reflection and (b) transmission spectra of r-GO and CGB films. (c) Reflection spectra of PTFE filter.

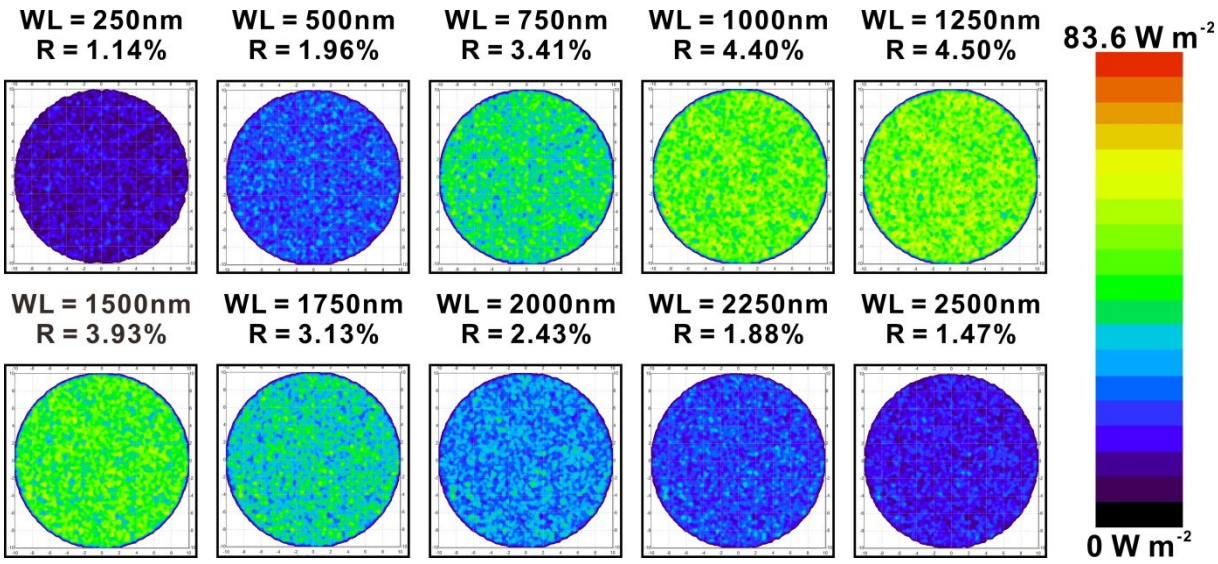

Figure S3. Simulation reflection distribution of the upper surface of the CGB800 film under one sun at different illuminating wavelength. The color scale on the right shows the level of light intensity of reflection.

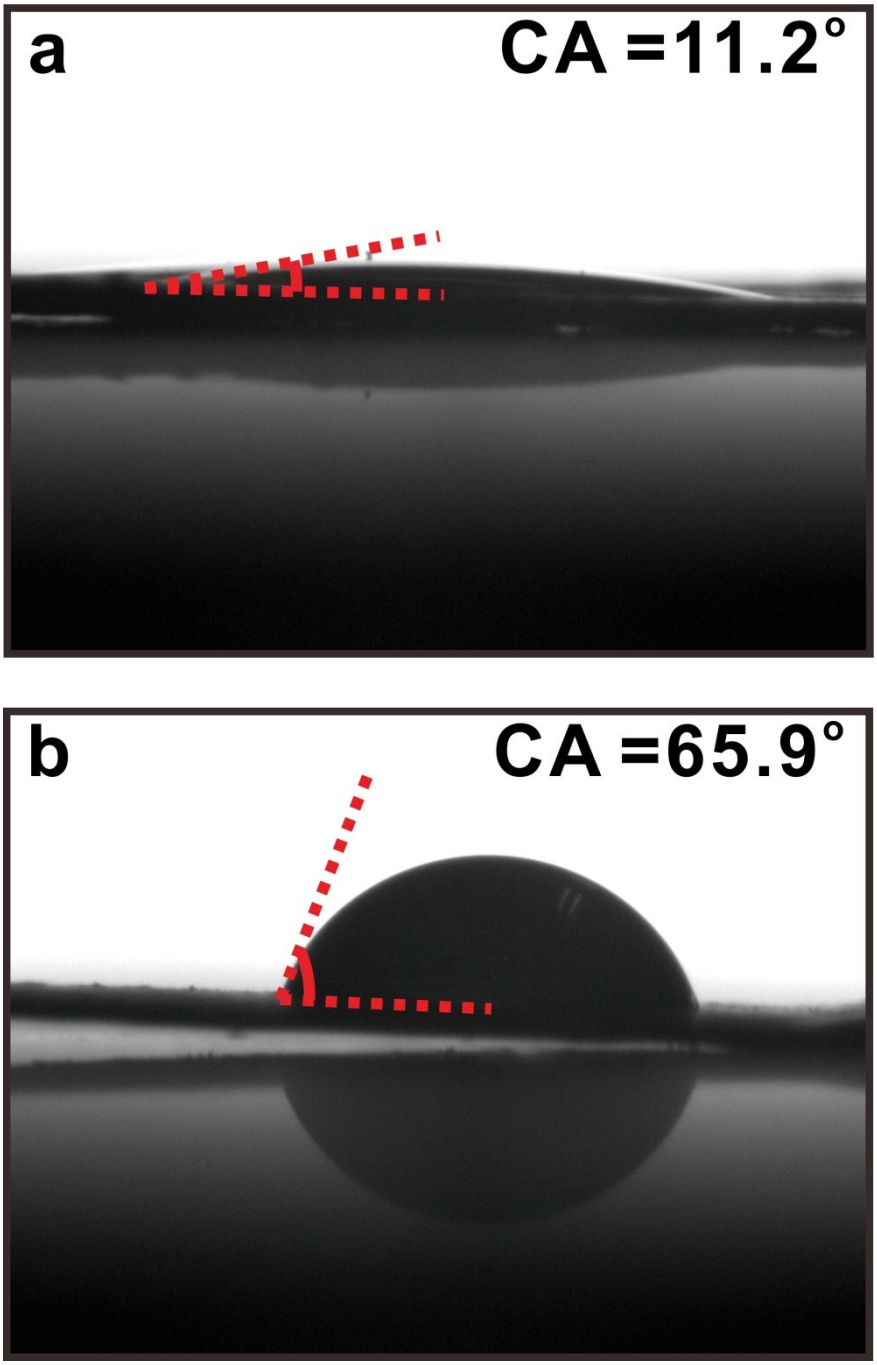

Figure S4. Contact angle (CA) of (a) CGB800 film at the beginning and (b) r-GO film.

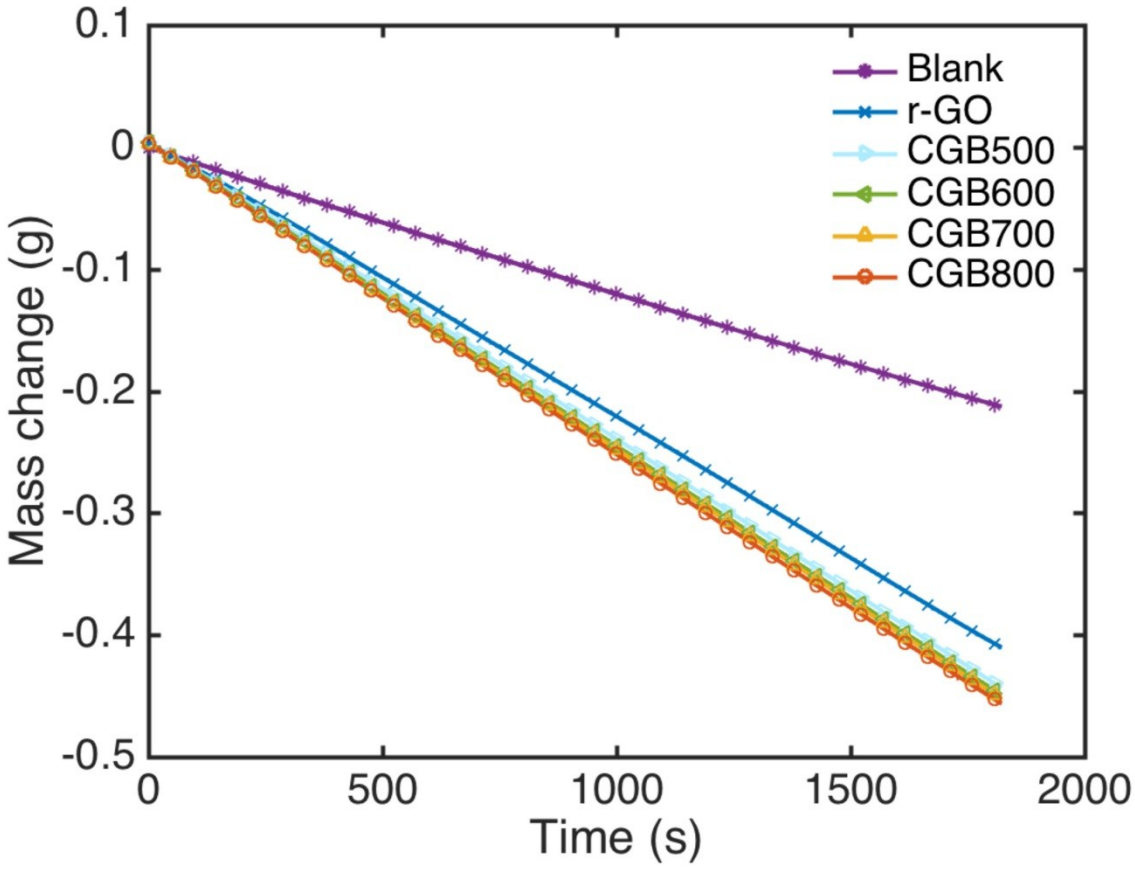

Figure S5. Mass changes over time in 0.5 h of evaporation using r-GO and CGB films.

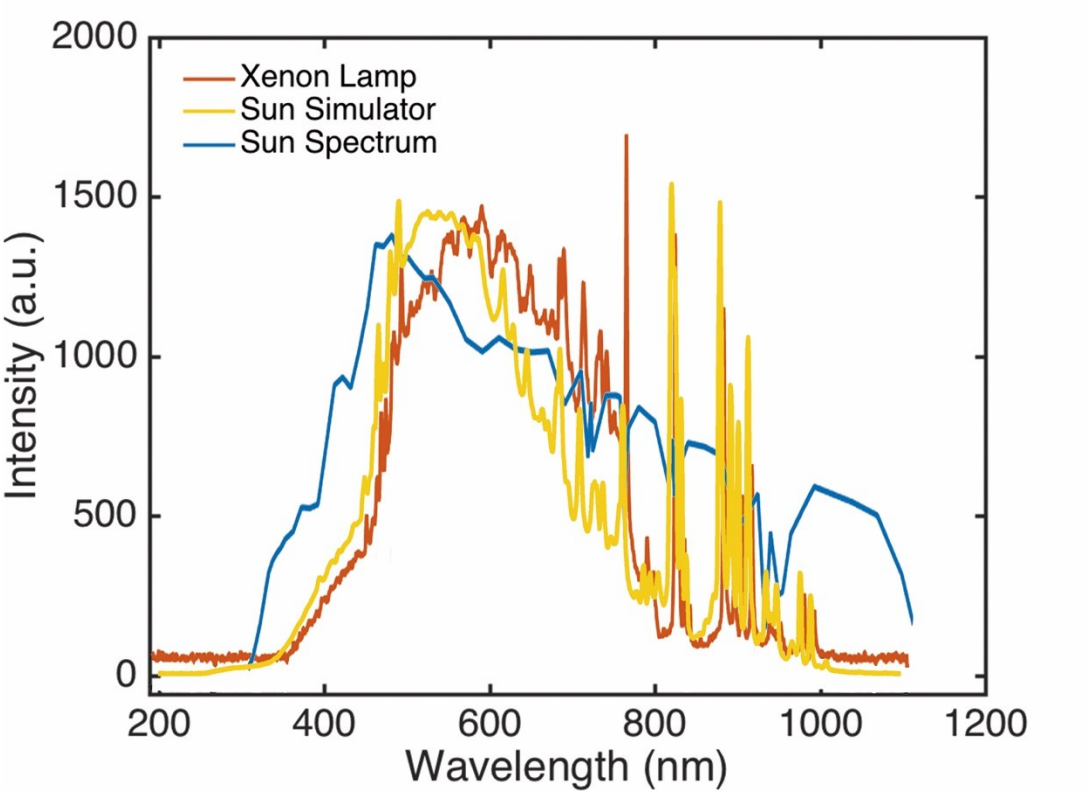

Figure S6. Spectra of the xenon lamp, sun simulator[4] and sun[5].

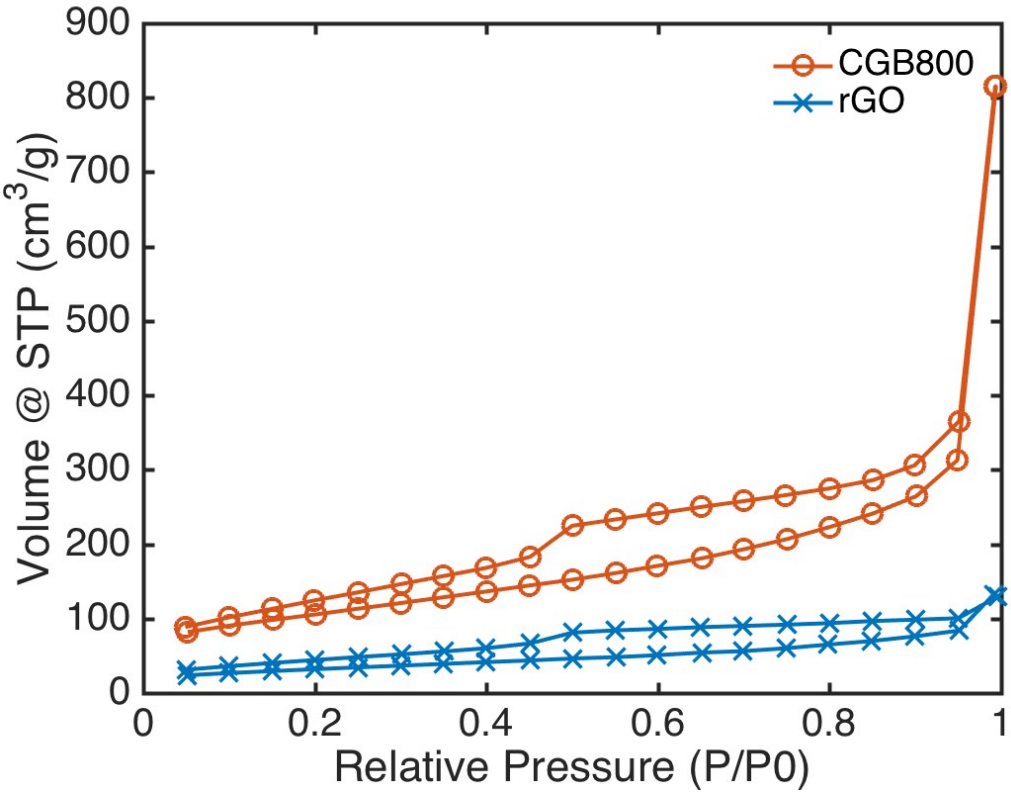

Figure S7. Volume over relative pressure of CGB800 film and rGO film.

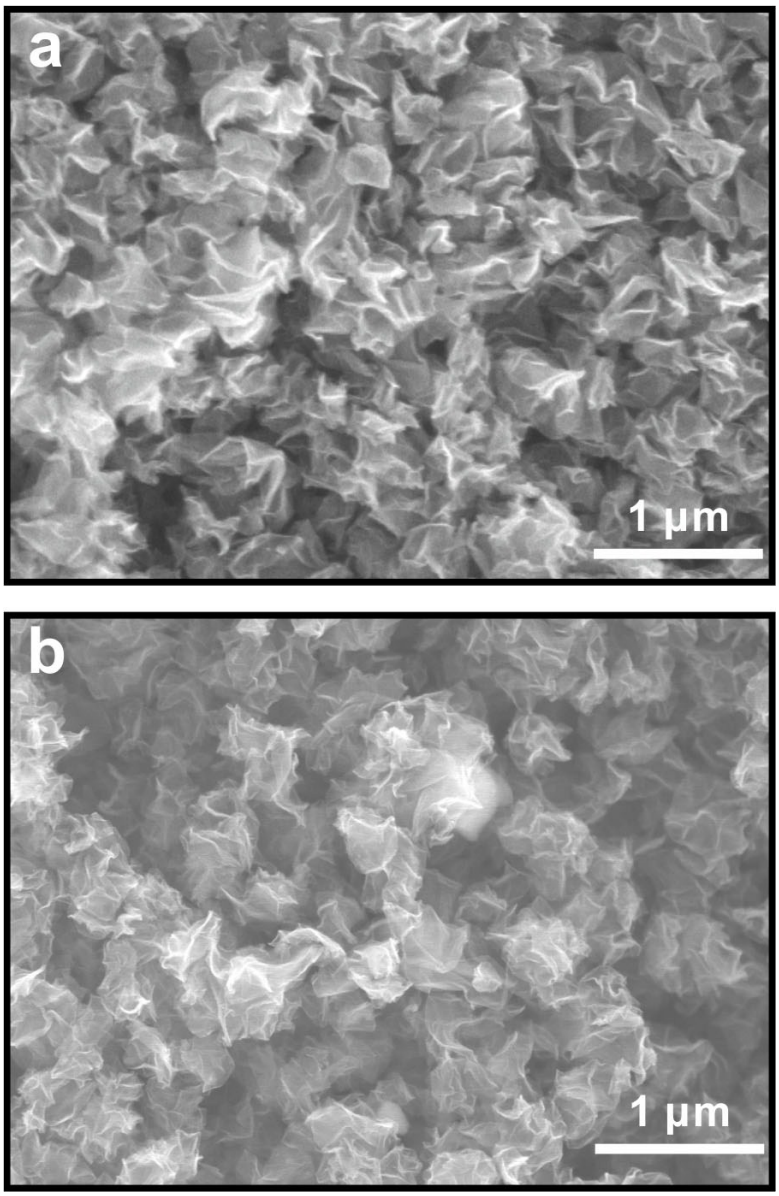

Figure S8. SEM images of CGB800 (a) before and (b) after evaporation cycling.

5. Additional References:

1 Casiraghi, C.; Hartschuh, A.; Lidorikis, E.; Qian, H.; Harutyunyan, H.; Gokus, T.; Novoselov, K. S.; Ferrari, A. C. Rayleigh Imaging of Graphene and Graphene Layers. *Nano Lett.* **2007,** *7*, 2711-2717.

2 Mätzler, C. MATLAB Functions for Mie Scattering and Absorption, Version 2. *IAP Res. Rep.* **2002,** *8*, 1.

3 van de Hulst, H. C. Light Scattering by Small Particles. Wiley, NewYork **1957**.

4 Chen, Y. Y.; Quan, X. J.; Wang, Z. Y.; Lee, C. S.; Wang, Z. Z.; Tao, P.; Song, C. Y.; Wu, J. B.; Shang, W.; Deng, T. Stably dispersed high-temperature Fe3O4/silicone-oil nanofluids for direct solar thermal energy harvesting. *J. Mater. Chem. A* **2016**, *4*, 17503.

5 Matson, R. J.; Emery, K. A.; Bird, R. E. Terrestrial solar spectra, solar simulation and solar cell short-circuit current calibration: a review. *Solar cells* **1984**, *11*, 105.